Nonlinear Viscoelastic Behavior of Wool Fibers in a Single Step Relaxation Test

F.-J. WORTMANN, *Deutsches Wollforschungsinstitut, D-51 Aachen, West Germany,* and S. DE JONG, *CSIRO Division of Textile Physics, Ryde, NSW 2112, Australia*

Synopsis

Experimental data and their analysis are presented on the nonlinear viscoelastic behavior of wool fibers in extensional stress–relaxation up to strains of 18.5%. The analysis, assuming a two-phase structure for the fiber, consists of superimposing the experimental curves onto the master curve for the nonaging material by multiplicative scaling and shifting on the log-time scale. The scaling and shift factors reflect the strain induced phase changes of the morphological components. Though different in their physical nature, these transitions show the same strain dependence.

INTRODUCTION

Wool fibers show linear viscoelastic (lve) behavior in extensional relaxation for strains up to approximately 0.8%,[1] close to the limit (1%) exhibited by a large number of other glassy polymers.[2] Above the lve–strain limit and for conditions below the glass transition,[3] comparatively little systematic information is available on the viscoelastic behavior of a wool fiber. This is unfortunate as strains outside the lve region are common in the processing of wool fibers[4] and might play a role in the performance of fibers in a fabric, e.g., in the wrinkling of a wool fabric.[5]

The aim of this article is to present experimental data on the nonlinear viscoelastic (nlve) behavior of wool in a single step relaxation test for extensions of up to 18.5%. The analysis of the data is based on Schapery's theory[6] in which the nlve response of the material is expressed in terms of its lve properties and certain functions of strain. The mechanical behavior and the change in behavior with strain in terms of the individual responses of the two major morphological components of a wool fiber is examined accordingly.

EXPERIMENTAL

Unmedullated Lincoln wool fibers without major diameter irregularities were chosen and washed in petroleum ether, ethanol, and water. The fibers were cut to 70 mm length and their diameter measured microscopically at 10 points along their length in water at 20°C.

All relaxation tests were made on the tensile tester described by Feughelman,[7] equipped with a motor to extend the fiber at a constant rate of strain. The fiber, the force pickup of the transducer, and the plug holder were enclosed in a double-walled glass chamber which contained a glycerol/

Journal of Applied Polymer Science, Vol. 30, 2195–2206 (1985)
 CCC 0021-8995/85/052195-12$04.00

water mixture (68% glycerol by weight), to maintain at 20°C 65% relative humidity (RH) above the solution.[8]

Before each test, the fibers were immersed in water at 50°C for 1 h. This treatment erases the mechanical and thermal history of the fibers, provided that the previous strains did not exceed 30%. The same fiber could hence be used repeatedly. Each fiber was brought to equilibrium with the environmental conditions by wetting, drying at 0% RH over pure glycerol for 1 h and then equilibrating overnight at 65% RH for 1000 min. The length of the fiber loop was 25 mm and was in all tests extended at a rate of 20%/min. The initial length was defined as the point of zero stress extrapolated from the linear proportion of the "Hookean" region of the stress–strain curve (Fig. 1). The curve shows that the fiber leaves the "Hookean" and enters the yield region around 2% strain.

All stress and moduli data are nominal values, based on the cross-sectional area of the fiber in water at 20°C. No correction for the influence of the crimp of the fiber on the determination of strain and hence of modulus was made.

RESULTS

After conditioning the specimen was strained to a predetermined value and the subsequent stress relaxation recorded. Figures 2 and 3 give the relaxation data for strains between $\epsilon = 0.5\%$ and $\epsilon = 18.5\%$. The data are represented as relative force, $F(t)/F(t_\epsilon)$, vs log time, where $F(t_\epsilon)$ is the force at the end of the straining step at t_ϵ. t_ϵ is taken as the zero time of the relaxation. Relative force values showed an inter- and intrafiber reproducibility of within 2%. Data measured over 3 decades of time between 10 s and 10,000 s were used for analysis (solid lines in Figs. 2 and 3). The data

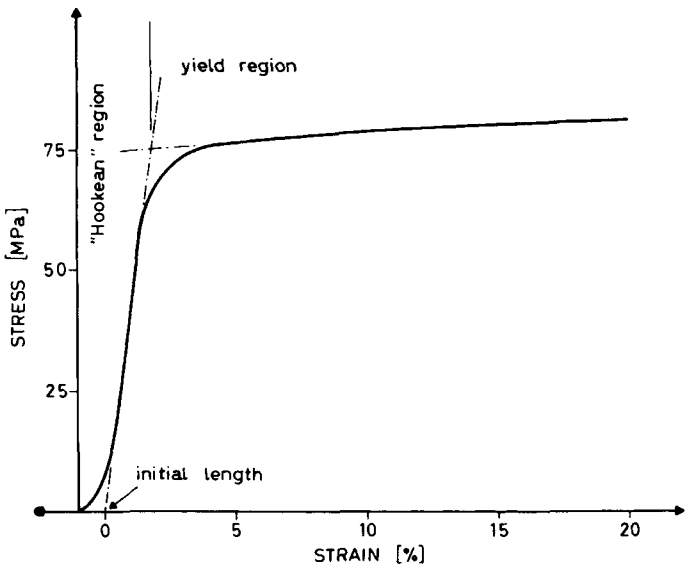

Fig. 1. The stress–strain curve of a wool fiber at 65% relative humidity. The terminology with respect to the curve is given.

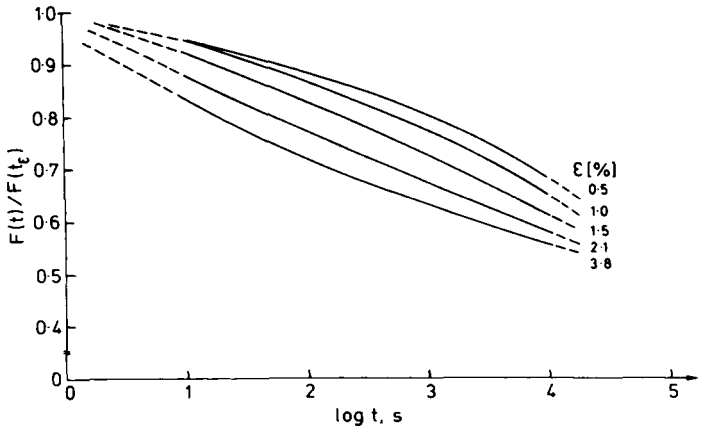

Fig. 2. Normalized relaxation curves for strains in the linear viscoelastic region and at the beginning of the yield region between $\epsilon = 0.5\%$ and $\epsilon = 3.8\%$. The normalizing factor $F(t_\epsilon)$ is the force at the end of the straining step.

for shorter times were ignored since they are, at least for strains in the "Hookean" region, influenced by the rate of straining. Data for longer times were not used due to effects outside the scope of this article, e.g., the aging of the wool fiber, the change of the aging rate with strain and the independent length change of the fiber with time. These effects interfere significantly with the objective of the experiment if the measuring time is appreciably greater than approximately 1/5 of the aging time.

Based on the cross-sectional area of the fibers in water (20°C), the value of the "Hookean" modulus of the fiber at 65% RH/20°C and in water/20°C was determined to be $E = 3.4$ GPa $\pm 10\%$ and $E = 1.7$ GPa $\pm 10\%$, respectively. The final stress relaxation modulus E_∞ ultimately reached after relaxation for long times at small strains is independent of the water content of the fiber.[1] Due to the acceleration of the relaxation in water E_∞ can be estimated from the curves as $E_\infty = 1.4$ GPa, in agreement with the literature data.[1]

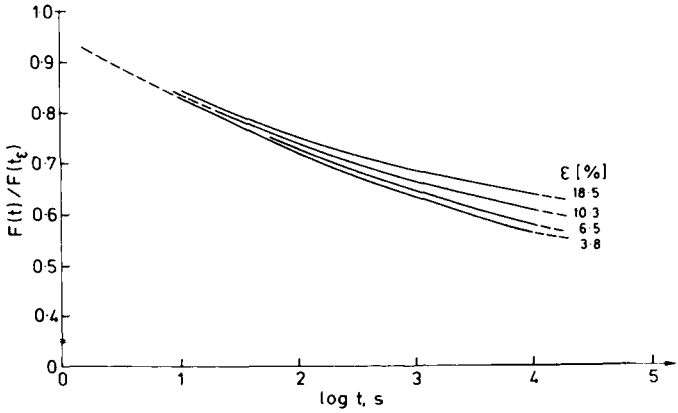

Fig. 3. Normalized relaxation curves for strains in the yield region between $\epsilon = 3.8\%$ and $\epsilon = 18.5\%$.

LINEAR AND NONLINEAR VISCOELASTICITY

The relaxation behavior of a wool fiber in the lve region can be described by a two-phase model[9] consisting of continuous, linearly elastic filaments (phase C) embedded in an amorphous viscoelastic material (phase M). Equation (1) represents this model in a form applicable to the stress relaxation of the nonaging fiber (a nonaging fiber is taken to be one whose properties do not change significantly during the course of the experiment):

$$E(t) = (E_0 - E_\infty) \cdot \Psi(t) + E_\infty$$

$E(t)$ = stress relaxation modulus

$E_0 \equiv E(0)$ = initial modulus (1)

$E_\infty \equiv E(\infty)$ = equilibrium or final value of modulus

$\Psi(t)$ = relaxation function with the property $\Psi(0) = 1$ and $\Psi(\infty) = 0$

This model is applicable for different modes of mechanical testing,[1,10,11] for the whole range of relative humidities[1] and other environmental conditions.[12] E_∞ is the contribution of the linearly elastic phase C to the stress–relaxation modulus. The appraisal of the morphology of the wool fiber[13] supports the view that the phase C represents the α-helical material in the fiber. Short α-helical segments in complex aggregates form continuous, axially oriented filaments[14] deforming linearly elastically up to strains of about 2% and in parallel with the whole fiber.

The amorphous phase M with the initial modulus $(E_0 - E_\infty)$ comprises all the noncrystalline morphological components of the fiber including the material traditionally referred to as matrix.

Several successful attempts have been made to describe the relaxation function for wool using the cumulative log-normal distribution[12,15,16] in the following expression:

$$\Psi(\ln t) = \frac{1}{[(2\pi)^{1/2}\beta]} \int_{\ln t}^{\infty} \exp\left[-\frac{1}{2}\left(\frac{x - \alpha}{\beta}\right)^2\right] dx \tag{2}$$

where α is the mean and β the standard deviation of the distribution.

For relaxations within the lve region the initial modulus E_0 is taken as equal to the experimental modulus of the fiber, since the curves show the neglegible effect of relaxation at short times. E_0 and E_∞ are thus measurable quantities. Rearrangement of eq. (1) for the ln time scale yields

$$\Psi(\ln t) = [E(\ln t) - E_\infty]/(E_0 - E_\infty) \tag{3}$$

Applying the principles of the usual graphical procedure,[17] a computer program was used to fit the cumulative log-normal distribution to the values of $\Psi(\ln t)$ for the lve relaxation curves, determining α and β (95% confidence limits) as

mean: $\alpha = 9.3_4 \pm 1\%$

standard deviation: $\beta = 5.2_9 \pm 3\%$

with $E_0 = 3.4$ GPa and $E_\infty = 1.4$ GPA so that $E_\infty/E_0 = 0.4$. The relaxation proceeds over approximately 9 decades of time and is represented by the solid line in Figure 4, as the curve of normalized stress vs. log time for the nonaging fiber. In what follows this curve will be referred to as the master curve, for an aging time of $t_A = 1000$ min.

The equation for nonlinear behavior is formulated on the basis of Schapery's theory[6]:

$$E(t,\epsilon) = h_1(\epsilon) \cdot E_\infty + h_2(\epsilon) \cdot (E_0 - E_\infty) \cdot \Psi(t/a_\epsilon(\epsilon)) \tag{4}$$

where $h_1(\epsilon)$ = strain function influencing the equilibrium modulus, $h_2(\epsilon)$ = strain function influencing the initial viscoelastic contribution, and $a_\epsilon(\epsilon)$ = shift factor, shifting the relaxation function on the log time scale.

For strains within the lve limits the relaxation behavior is independent of strain and the strain functions, and the shift factor become unity, i.e., $h_1 = h_2 = a_\epsilon = 1$ and eq. (4) transforms into eq. (1). The introduction of the reduced time through the strain dependent shift factor a_ϵ implies that the strains outside the lve limits act on all relaxation times in exactly the same way, producing on the log-time scale a lateral shift of the relaxation function.

ANALYSIS

The analysis which proved successful in providing a good fit for the data as well as yielding information on the performance of the morphological components consisted of superimposing the experimental curves onto the master curve by applying a multiplicative scaling factor, the singular strain function $h(\epsilon)$, and a shift factor $a_\epsilon(\epsilon)$, simplifying eq. (4) to

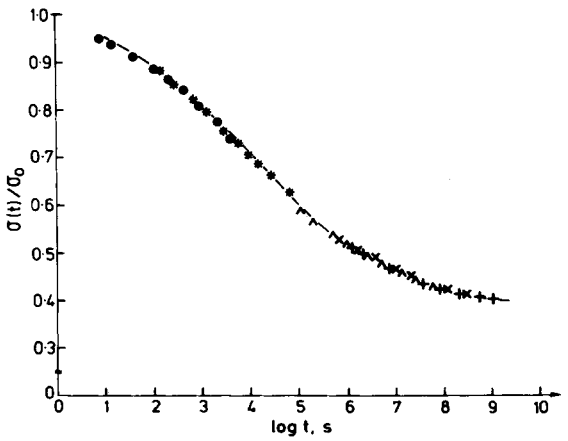

Fig. 4. Normalized relaxation master curve for the nonageing fiber. The various points are from the relaxation curves for the strains indicated, suitably shifted and scaled. ϵ (%): (●) 0.5; (✱) 2.1; (^) 3.2; (×) 10.3; (+) 18.5.

$$E(t,\epsilon) = h(\epsilon)\,[E_\infty + (E_0 - E_\infty) \cdot \Psi(t/a_\epsilon(\epsilon))] \tag{5}$$

In a double logarithmic plot of $E(t,\epsilon)$ vs. t, the curves can be superimposed onto the master curve by shifting them along the two axes, the amounts of vertical and horizontal shift yielding $h(\epsilon)$ and $a_\epsilon(\epsilon)$, respectively. Since this graphical method is not very sensitive, the following superposition procedure for the determination of $h(\epsilon)$ and $a_\epsilon(\epsilon)$ was employed. The normalized master curve, $E(t)/E_0$ vs. log t, is shifted horizontally against the normalized experimental relaxation curve, $F(t)/F(t_\epsilon)$ vs. log t. For a given shift, log a, the isochronal points of the two curves are analyzed in a linear regression forced through the origin. $K(\epsilon)$ is the slope of the regression line:

$$\frac{F(t)}{F(t_\epsilon)} = K(\epsilon) \cdot \frac{E(t/a)}{E_0} \tag{6}$$

The optimal shift factor $a_\epsilon(\epsilon)$ is found by varying a to find the best fitting linear regression. The fits achieved in this way were very satisfactory. The largest deviation of any of the experimental points from the master curve after shifting and scaling was smaller than 2%. Figure 4 shows how the scaled and shifted experimental curves fit onto the master curve.

In Figure 5 the shift factor is plotted vs. strain on a double log scale. Figure 6 gives the values of the slope of the regression line $K(\epsilon)$ vs. log strain. Both figures show around $\epsilon = 2.5\%$ a major jump indicating an abrupt change in the mechanical properties of the fiber. For t = 0 it follows from eq. (6) that

$$F(0) = F(t_\epsilon) \cdot K(\epsilon) \tag{7}$$

and

$$\sigma_0 \equiv \sigma(0) = \sigma(t_\epsilon) \cdot K(\epsilon) \tag{8}$$

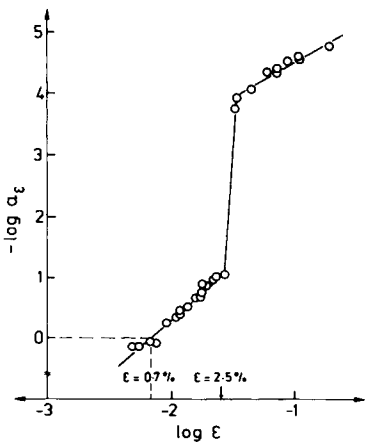

Fig. 5. Double logarithmic plot of shift factor vs. strain. The limit of the lve region and the strain at the start of the discontinuity are indicated.

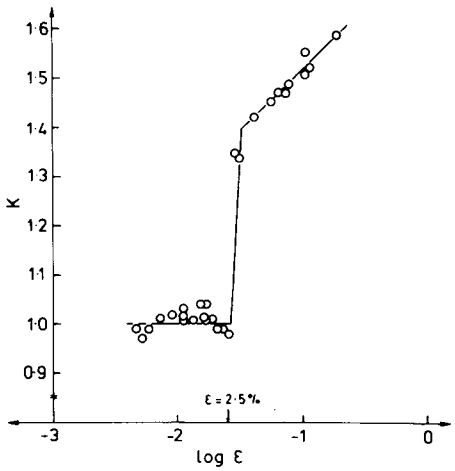

Fig. 6. Slope of the origin regression line between master and experimental curves K vs. log strain. The strain at the discontinuity is indicated.

where σ_0 is the stress that would be reached for a given strain in the absence of stress relaxation.

With eq. (8) the influence of stress–relaxation on the experimental stress–strain curve can be compensated to calculate the isochronal, zero-time stress–strain curve of the fiber, σ_0 vs. ϵ. Using the strain-invariant ratio of the initial and equilibrium moduli and hence stresses, $\sigma_\infty/\sigma_0 = 0.4$, the contributions of the two morphological components, the phase C,σ_∞ vs. ϵ, and the phase M, $(\sigma_0, - \sigma_\infty)$ vs. ϵ, can be separated. Figure 7 shows these curves and the experimental stress–strain curve, $\sigma(t_\epsilon)$ vs. ϵ.

The ratio σ_0/ϵ gives the modulus of the fiber at all extensions, which is related to the initial modulus in the lve region E_0 through the strain function:

$$\sigma_0/\epsilon = h(\epsilon) \cdot E_0 \tag{9}$$

Figure 8 shows the strain function derived from the data in Figure 7 and its marked change when the fiber enters the yield region.

DISCUSSION

The description of the stress–relaxation behavior of the wool fiber in the linear viscoelastic region was extended to yield a satisfactory quantitative description of the nonlinear viscoelastic behavior. The extension consisted of introducing a single strain function, acting on the elastic and viscoelastic phase alike, and a time shift factor. The morphological components, the crystalline α-helices, and the surrounding amorphous phase exhibit transitions distinctly different in nature. Up to approximately 2% strain, the α-helices deform in parallel with the whole fiber. At higher strains they undergo a transition possibly of first order,[18] from the α-helical to the β-pleated sheet structure at nearly constant stress. This transition allows for any α-helical segment opening up into the β-form a length change of 125%.[11] The shape of the strain function reflects this transition of the filaments

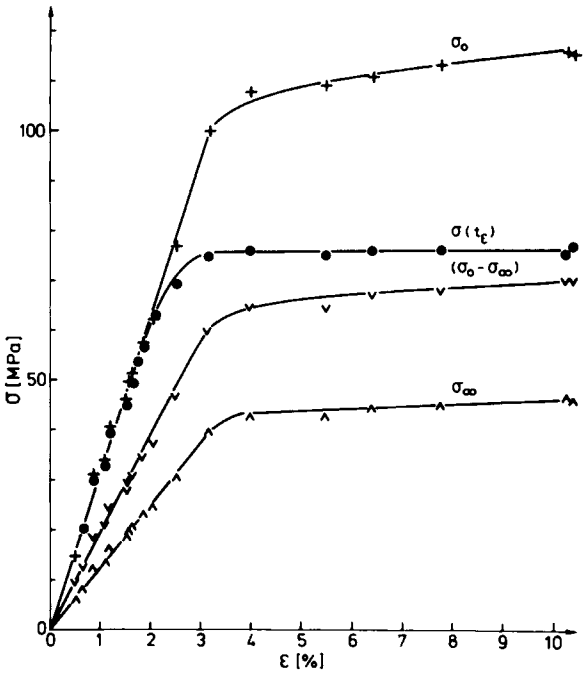

Fig. 7. Experimental, $\sigma(t_\epsilon)$, and isochronal, zero-time stress–strain curve of the fiber, σ_0, and of the morphological components phase C, σ_∞, and phase M, $(\sigma_0 - \sigma_\infty)$.

with strain. Much less is known about the mechanical properties of the phase M. The experimental evidence in general indicates that it behaves like a glassy, amorphous polymer, nearly elastic for normal strain rates at small strains ($\epsilon < 1\%$) and going into continuous flow in the yield region ($\epsilon > 2$–3%).[11] The changes of the mechanical properties of the phase M with strain are reflected in $h(\epsilon)$ as well as in $a_\epsilon(\epsilon)$.

The singularity of the strain function is probably not coincidental but due to a causality between the transitions of the phases, acting in parallel

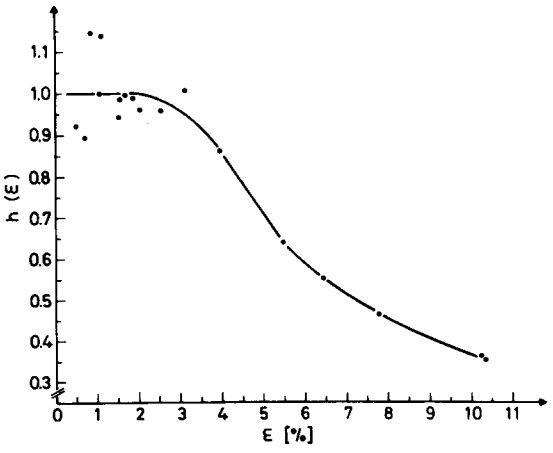

Fig. 8. The strain function $h(\epsilon)$ vs. strain.

at all strains. The length increase for an individual α-helical segment going from the α into the β form will impose such a high, localized stress in the surrounding phase M that a solid/fluid transition is initiated.

Figure 5 shows that the position of the relaxation function on the log-time scale is unchanged in the lve region ($\log a_\epsilon \simeq 0$) for $\epsilon < 0.7$). Beyond this region a shift to shorter times linear with log strain as well as approximately linear with linear strain occurs. The shift rate of 1 decade of time/1.8% strain at strains below 2.5% is in reasonable agreement with Ferry and Stratton's prediction[19] of 1 decade/1% strain, based on free volume theory.

At the changeover from the "Hookean" into the yield region there is a jump in the values of a_ϵ shifting the relaxation function between 2% and 3% strain by 3 decades to shorter times. This can be interpreted as a deaging of the fiber.[20] Wool fibers age at strains in the lve region in very much the same way as other materials, their relaxation curves shifting to longer times on the log time scale by 1 decade/decade of aging time.[21] The shift of the relaxation function by overall 4 decades reduces the initial aging time $t_A = 1000$ min effectively to $t_A = 0.1$ min equivalent to a virtually complete deaging. For a glassy polymer this usually is achieved by heating to a temperature above the glass transition. This equivalence of strain and temperature supports the idea that the molecular flow in the yield region is permitted when the applied strain has generated free volume to an extent characteristic for the polymer above the glass transition.[22] For strains in the yield region the shift rate with strain drops considerably to about 1 decade/20% strain, so that the relaxation behavior is largely independent of strain.

Unlike the shift factor a_ϵ the value of K is independent of strain up to strains well outside the lve region, where around $\epsilon = 2.5\%$ a discontinuity occurs. K is a measure of the occurrence of stress–relaxation during the straining step and gives the relation between the experimental stress–strain curve, $\sigma(t_\epsilon)$ vs. ϵ, and the isochronal stress–strain curve, σ_0 vs. ϵ (Fig. 7). For small strains where $K = 1$, virtually no stress–relaxation occurs during the straining step and $F(t_\epsilon)$ is a direct measure of the elastic modulus E_0. $K > 1$ indicates that stress–relaxation becomes a significant event during straining. This happens when at the discontinuity of $\log a_\epsilon$ the mean relaxation time drops by 4 orders of magnitude into the range of the straining time. Beyond the discontinuity that occurs around $\epsilon = 3\%$ when strains in the yield region are reached, $K(\epsilon)$ changes linearly with log strain by 0.26/decade strain.

By subtracting the stress–strain curve of the phase C, σ_∞ vs. ϵ, from the experimental stress–strain curve, $\sigma(t_\epsilon)$ vs. ϵ, the experimental stress–strain curve of the phase M is obtained. Figure 9 shows this curve as well as the isochronal stress–strain curve of the phase M, $(\sigma_0 - \sigma_\infty)$ vs. ϵ (from Fig. 7). The difference between the two curves, $[\sigma_0 - \sigma(t_\epsilon)]$ vs. ϵ, represents the loss of stress in the phase M due to stress–relaxation during straining. This difference curve is shown in Figure 9 and indicates the rapid loss of stress in the transition region in parallel with the change of the shift factor and the value of K with strain. The experimental stress–strain curve for the phase M, $[\sigma(t_\epsilon) - \sigma_\infty]$ vs. ϵ, shows a distinct maximum, marking the yield

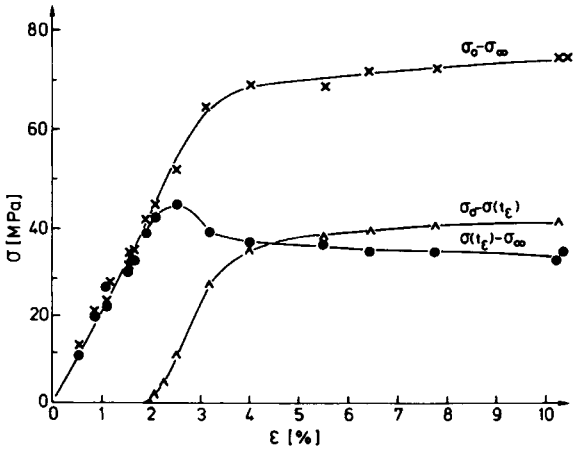

Fig. 9. The isochronal, $(\sigma_0 - \sigma_\infty)$, and the experimental stress–strain curve, $[\sigma(t_\epsilon) - \sigma_\infty]$, of the phase M. $[\sigma_0 - \sigma(t_\epsilon)]$ represents the change of stress in the phase M due to the shift of the relaxation curve with strain.

point around 2–3% strain, and a subsequent continuous decrease of stress with increasing strain. An analogous phenomenon is commonly observed in "strain-softening" polymers.

The occurrence of a solid/fluid transition on yielding can be substantiated by calculating the viscosity of the phase M on both sides of the yield point. In the lve region the Newtonian viscosity of the phase M in extension is given by[16]

$$\eta = t^* \cdot (E_0 - E_\infty) \exp(\beta^2/2 + \alpha), \quad t^* = 1 \text{ s} \tag{10}$$

Considering eqs. (1) and (4) this generalizes for nlve behavior to

$$\eta = t^* \cdot h(\epsilon) \cdot a_\epsilon(\epsilon) \cdot (E_0 - E_\infty) \cdot \exp(\beta^2/2 + \alpha) \tag{11}$$

For lve behavior, eq. (10) and the data given in the viscoelastic section yield a viscosity in the range of

$$\eta \simeq 10^{19} \text{ Pa}$$

This value greatly exceeds $\eta = 10^{14}$ Pa, which is the value generally used to distinguish between solids and fluids. For strains in the yield region the viscosity decreases mainly due to the drastic drop of the shift factor. Equation (11) applied to the data given above yields a viscosity depending on the strain in the yield region in the range of

$$\eta = 10^{14}\text{–}10^{15} \text{ Pa}$$

In the yield region the viscosity drops into the range of highly viscous fluids or soft solids, which allows the phase M to accomodate to strains, where the hard solid would have broken. This is confirmed by the fact that wool fibers in liquid nitrogen, $T = 196$°C, where all viscous mechanisms are

suppressed, break at strains of 3%[23] in close agreement with the yield point at 2.5% strain (Fig. 9).

For the first 2–3% strain the strain function is unity, and the deviation from linear behavior is only determined by the shift factor a_ϵ, so that nonlinear effects are limited to the phase M. Equation (4) thus reduces to

$$E(t,\epsilon) = E_\infty + (E_0 - E_\infty)\Psi(t/a_\epsilon(\epsilon)) \tag{12}$$

This region of small strains where eq. (12) applies is of special interest, since it represents the bending strains (≈2%) of a fiber in a fabric subjected to the standard wrinkling test.[24] These strains can be expected to shift the relaxation curve and hence "deage" the fiber by 1 decade of time. Chapman[25] showed for the recovery of Merino wool fibers from 2% bending strain an absolute increase of setup to 5% compared to the values calculated by using lve theory. In a similar way to a reduced aging state of the fiber,[21] the nlve effects thus increase the set of the fiber compared to the set expected at lower strains and possibly contribute to that difference between the predicted and the measured recovery of wool fabrics presently attributed to a frictional component.[26]

This work was supported by the Australian Wool Research Trust Fund, by the International Wool Secretariat, by the Forschungskuratorium Gesamttextil (AIF No. 4972), the funds being provided by the Bundeswirtschaftsministerium via the Arbeitsgemeinschaft Industrieller Forschungsvereinigungen (AIF) and also by the Ministerium für Wissenschaft und Forschung des Landes Nordrhein-Westfalen. The assistance provided by Miss E. Yakuner in carrying out the experimental work is also greatly appreciated.

References

1. M. Feughelman and M. S. Robinson, *Text. Res. J.*, **41**, 469 (1971).
2. I. V. Yannas, *J. Polym. Sci., Macromol. Rev.*, **9**, 163 (1974).
3. F.-J. Wortmann, B. J. Rigby, and D. G. Phillips, *Text. Res. J.*, **54**, 6 (1984).
4. K. Baird, *Text. Res. J.*, **45**, 442 (1975).
5. E. F. Denby, *J. Text. Inst.*, **65**, 250 (1974).
6. R. A. Schapery, *Polym. Eng. Sci.*, **9**, 295 (1969).
7. M. Feughelman, *Text. Res. J.*, **29**, 967 (1959).
8. C. S. Miner and N. N. Dalton, Eds., *Glycerol*, Reinhold, New York, 1953.
9. M. Feughelman, *Text. Res. J.*, **29**, 223 (1959).
10. B. M. Chapman, *J. Text. Inst.*, **66**, 343 (1975).
11. G. Danilatos and M. Feughelman, *Text. Res. J.*, **50**, 568 (1980).
12. F.-J. Wortmann and H. Zahn, *Proc. 6th Int. Wool Text. Res. Conf. Pretoria* **II**, 323 (1980).
13. E. G. Bendit and M. Feughelman, "Keratin," *Encyclopedia of Polymer Science and Technology*, Wiley, New York, 1968, Vol. 8, p. 1.
14. R. D. B. Fraser, T. P. MacRae, and E. Suzuki, *J. Molek. Biol.*, **108**, 435 (1976).
15. G. D. Danilatos, PhD thesis, University of NSW, Sydney, 1977.
16. F. H. Stootman, PhD thesis, University of NSW, Sydney, 1977.
17. H. J. Henning and P.-Th. Wilrich, *Statistische Methoden bei textilen Untersuchungen*, 2nd ed., Springer-Verlag, Berlin, 1974.
18. A. Cifferi, *Trans. Faraday Soc.* **59**, 562 (1963).
19. J. D. Ferry and R. A. Stratton, *Kolloid Z.*, **171**, 107 (1960).
20. L. C. E. Struik, *Physical Ageing in Amorphous Polymers and Other Materials*, Elsevier, Amsterdam, 1978.
21. B. M. Chapman, *Rheol. Acta*, **14**, 466 (1975).
22. K. C. Rusch and R. H. Beck, *J. Makrom. Sci., Phys.*, **B4**, 621 (1970).

23. M. Feughelman and M. S. Robinson, *Text. Res. J.*, **37**, 705 (1967).
24. E. F. Denby, *J. Text. Inst.*, **65**, 239 (1974).
25. B. M. Chapman, *J. Appl. Polym. Sci.*, **17**, 1693 (1973).
26. E. F. Denby, *J. Text. Inst.*, **71**, 201 (1980).

Received April 20, 1984
Accepted September 17, 1984